Research Article **Open Access**

Bosko M. Stojanovski, Leslie A. Pelc, Xiaobing Zuo, Nicola Pozzi, Enrico Di Cera*

Enhancing the anticoagulant profile of meizothrombin

https://doi.org/10.1515/bmc-2018-0016
received September 27, 2018; accepted November 19, 2018.

Abstract: Meizothrombin is an active intermediate generated during the proteolytic activation of prothrombin to thrombin in the penultimate step of the coagulation cascade. Structurally, meizothrombin differs from thrombin because it retains the auxiliary Gla domain and two kringles. Functionally, meizothrombin shares with thrombin the ability to cleave procoagulant (fibrinogen), prothrombotic (PAR1) and anticoagulant (protein C) substrates, although its specificity toward fibrinogen and PAR1 is less pronounced. In this study we report information on the structural architecture of meizothrombin resolved by SAXS and single molecule FRET as an elongated arrangement of its individual domains. In addition, we show the properties of a meizothrombin construct analogous to the anticoagulant thrombin mutant W215A/E217A currently in Phase I for the treatment of thrombotic complications and stroke. The findings reveal new structural and functional aspects of meizothrombin that advance our understanding of a key intermediate of the prothrombin activation pathway.

Keywords: Thrombin; Protein Engineering; Enzyme Specificity.

Introduction

Meizothrombin (Mz) is an important physiological intermediate generated during the proteolytic conversion of prothrombin into thrombin in the penultimate step of the coagulation cascade [1-7]. The prothrombinase complex, composed of factor Xa, cofactor Va, Ca^{2+} and phospholipids, cleaves prothrombin at two sites, R271 and R320, leading to the formation of the inactive precursor prethrombin-2 and the active intermediate Mz, respectively [1, 8, 9]. Importantly, the cleavage at R271 sheds the auxiliary domains of prothrombin, i.e., the Gla domain and the two kringles. On the other hand, the alternative cleavage at R320 initiates folding of the protease domain leading to enzymatic activity, while maintaining the multidomain architecture of the product intact and similar to that of the zymogen precursor prothrombin. Hence, Mz carries an active protease domain equivalent to thrombin linked covalently to the auxiliary domains of prothrombin. As such, Mz is an interesting intermediate of the prothrombin activation pathway, encouraging analysis of its multidomain architecture compared to prothrombin and of its enzymatic properties compared to thrombin.

The three-dimensional architecture of full length Mz remains unknown and the only current structures are those of human [10] and bovine [11] Mz lacking the Gla domain and kringle-1. Recent advances on the structure of prothrombin [12-16] have revealed two major conformations in equilibrium, open and closed, whose distribution changes upon interaction with prothrombinase. Under physiological conditions, prothrombin circulates mainly in the closed conformation, where kringle-1 docks onto the protease domain by intramolecular collapse. Binding of prothrombin to prothrombinase in the closed conformation exposes R320 for cleavage to generate meizothrombin, which then assumes an open conformation promoting cleavage at R271, shedding of the auxiliary domains and generation of thrombin [16]. Mz is not only a substrate of prothrombinase, bearing the same multidomain architecture as prothrombin, but is also an enzyme with functional properties similar to thrombin. Indeed, Mz cleaves fibrinogen to promote formation of a fibrin clot and triggers platelet aggregation by cleavage of PAR1, although the relative velocities measured for these procoagulant and prothrombotic substrates are significantly reduced in comparison to thrombin [3, 5, 17-21]. In contrast, Mz initiates the anticoagulant pathway by activating protein C upon interaction with the endothelial

***Corresponding author: Enrico Di Cera,** Edward A. Doisy Department of Biochemistry and Molecular Biology, Saint Louis University School of Medicine, St. Louis, MO 63104 USA, E-mail: enrico@slu.edu
Bosko M. Stojanovski, Leslie A. Pelc, Nicola Pozzi: Edward A. Doisy Department of Biochemistry and Molecular Biology, Saint Louis University School of Medicine, St. Louis, MO 63104 USA
Xiaobing Zuo: X-Ray Science Division, Argonne National Laboratory, Argonne, Illinois 60439

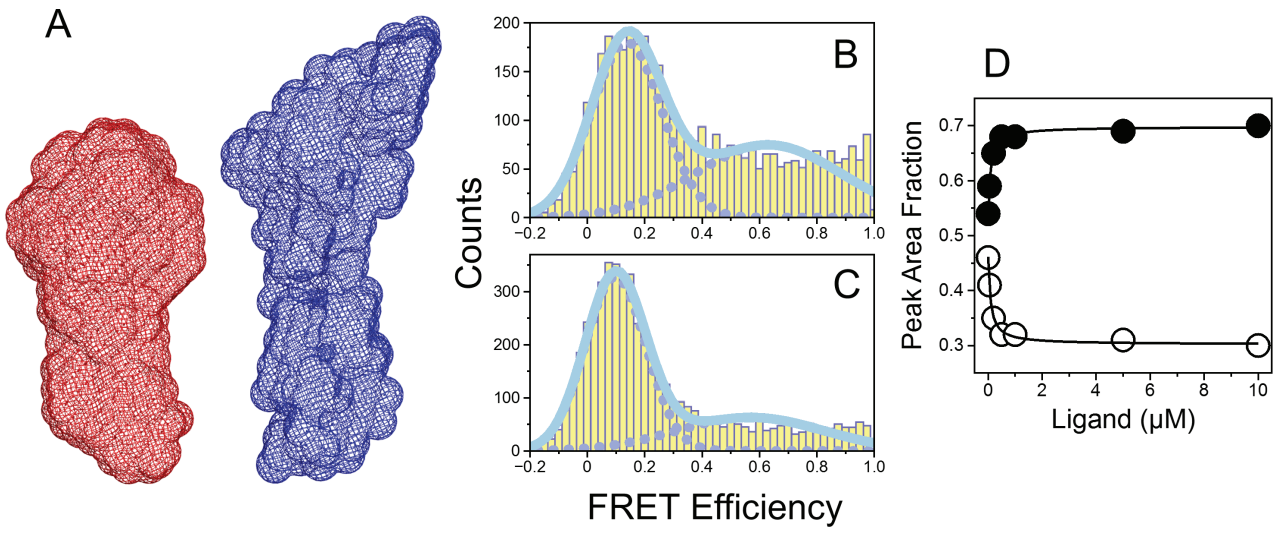

Figure 1A-D. Solution structures of prothrombin and Mz revealed by SAXS and smFRET measurements. (A) Reconstructed 3D envelopes of prothrombin (red) and Mz (blue) calculated from their respective scattering profiles. The maximal particle sizes (D_{max}) for prothrombin and Mz calculated from the pair distance distribution functions (not shown) are 120 Å and 160 Å, respectively. FRET efficiency histogram of Mz S525A labeled with the AF555/AF647 fluorophores at positions S120C/S478C measured in the absence (B) or presence(C) of saturating concentrations of H-D-Phe-Pro-Arg-p-nitroanilide (FPR). (D) Fractions of Mz molecules populating either the open (closed circles) or closed (open circles) conformations calculated at different concentrations of FPR. The K_d value for the interaction of Mz with FPR obtained from fitting the data into a single site model was 90±10 nM.

receptor thrombomodulin more efficiently than thrombin, due to the accelerating effect that phospholipids have on its anticoagulant function [18-20, 22]. Phospholipids also accelerate the activation of FV [23] and FXI [24] by Mz, as well as its intermolecular autoconversion into thrombin [25]. Importantly, the aforementioned catalytic properties implicate that Mz may function as a better anticoagulant enzyme than thrombin due to reduced activity toward procoagulant (fibrinogen) and prothrombotic (PAR1) substrates, linked to a slightly more pronounced activity toward the anticoagulant protein C in the presence of phospholipids [18, 19]. In murine models, direct infusion of a prothrombin variant activated to a stable form of Mz, delays carotid artery thrombosis more efficiently than injection of wild-type prothrombin that ultimately converts to thrombin [20].

In this study, we report new details on the structure and function of Mz. We use small angle X-ray scattering (SAXS) and single molecule Förster resonance energy transfer (smFRET) to unravel features of the conformation of this intermediate that can be compared to those recently reported for prothrombin [12, 13, 15, 16]. In addition, we characterize an engineered mutant of Mz in the context of the anticoagulant W215A/E217A (WE) mutant of thrombin [26-28] currently in Phase I for the treatment of thrombotic complications and stroke.

Results And Discussion

Recent X-ray and smFRET measurements have revealed a pre-existing equilibrium between closed and open conformations of prothrombin [12, 13, 15, 16]. The closed form predominates under physiological conditions and features an intramolecular collapse of kringle-1 onto the active site of the protease domain. Analogous measurements of Mz confirm the existence of two forms in equilibrium, but with the distribution shifted in favor of the open form. SAXS measurements of Mz in solution reveal an elongated shape (Figure 1A), with a maximal particle size (D_{max}) value of 160 Å, or 40 Å longer than that of prothrombin. Cleavage at R320 in the protease domain is therefore sufficient to weaken the intramolecular contact that stabilizes the closed form. This is consistent with recent findings from rapid kinetics measurements of ligand binding to the active site of thrombin, Mz and their zymogen precursors prethrombin-2, prethrombin-1 and prothrombin [29]. Formation of the H-bond between the newly formed N-terminus at residue I321 and the highly conserved D524 next to the catalytic S525 proceeds according to the celebrated Huber-Bode mechanism of zymogen activation [30]. The mechanism promotes ligand binding to the active site by reducing the rate of dissociation and shifting the conformational ensemble in favor of the open form [29]. New smFRET measurements

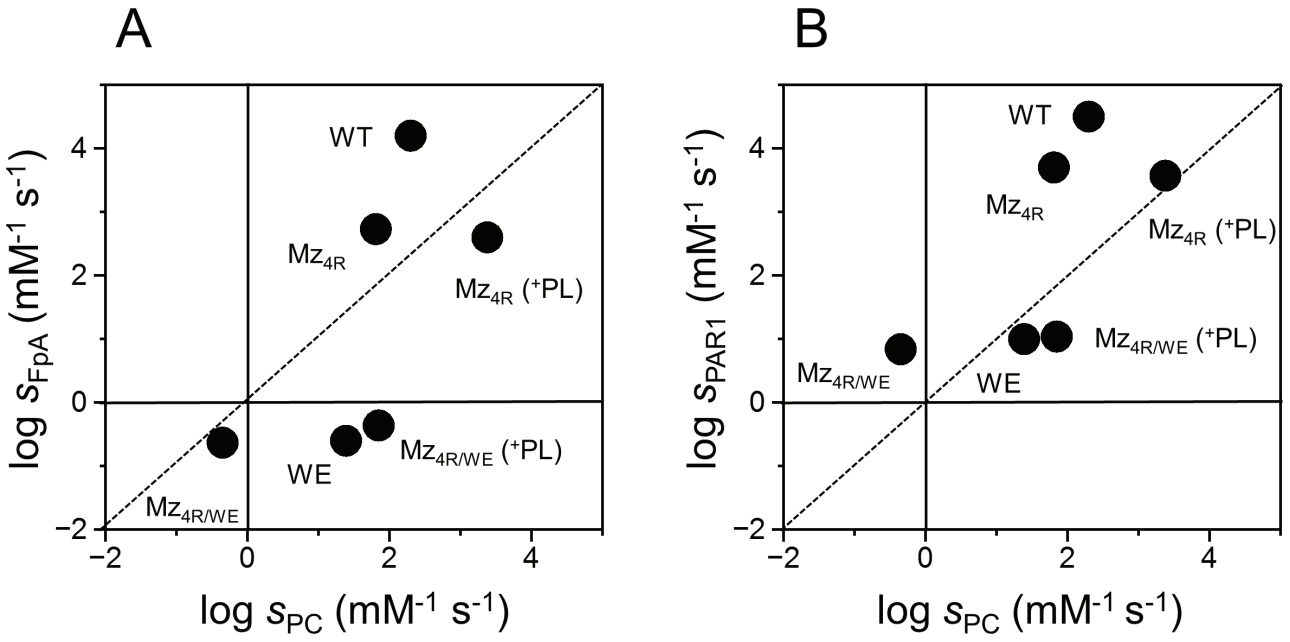

Figure 2A-B. Two dimensional plots of Mz and thrombin activities. Values of $s=k_{cat}/K_m$ for cleavage of fibrinogen (s_{FpA}) (A) or PAR1 (s_{PAR1}) (B) are plotted vs those for protein C (s_{PC}) activation. The region below the diagonal dotted line denotes activity toward protein C that exceeds that for fibrinogen (A) or PAR1 (B). The reverse is true for the region above the diagonal line. Phospholipids (PL) at a saturating concentration of 0.5 mM (see also Figure 3) selectively enhance the activity of Mz (Mz_{4R} or $Mz_{4R/WE}$) toward protein C, without affecting the rates of fibrinogen and PAR1 cleavage. The WE mutation profoundly decreases the activity of thrombin (WE) and Mz ($Mz_{4R/WE}$) toward fibrinogen and PAR1. Addition of phospholipids completely restores the activity of $Mz_{4R/WE}$ toward protein C and produces a significant anticoagulant effect that slightly exceeds that of the thrombin mutant WE. Values for wild-type (WT) and WE (WE) thrombin are from ref. [45].

of Mz also support the predominance of the open form for this intermediate (Figure 1B). Binding of a ligand to the active site shifts the distribution further in favor of the open form, but without significantly altering the relative FRET efficiency (Figure 1C). This is in agreement with conformational transitions of Mz that precede rather than follow the binding step, as predicted by the binding mechanism of conformational selection [29, 31].

To characterize the catalytic properties of Mz, we have engineered a derivative of the enzyme where residues R55, R155, R271 and R284 known to be susceptible to proteolysis [18, 32] were replaced with Ala. The resulting quadruple mutant R55A/R155A/R271A/R284A (Mz_{4R}) differs from previously characterized variants [18-20] insofar, as it includes the R55A mutation that enhances stability by preventing loss of the Gla domain by proteolytic cleavage [25, 32]. Mz_{4R} cleaves fibrinogen and a fragment of PAR1 with specificity constants higher than that measured for cleavage of protein C in the presence of thrombomodulin (Table 1, Figure 2). The preference, however, is significantly smaller than that seen for thrombin [28], especially in the case of fibrinogen. The origin of this difference is likely due to occupancy of exosite II by kringle-2 in Mz [10, 11] that masks epitopes responsible for the interaction with fibrinogen [28]. Exosite II is also important for binding of thrombomodulin [33], which could explain the reduced specificity constant of Mz toward protein C in the presence of cofactor. Furthermore, the presence of Gla domain in Mz has been reported to have a profound effect on the activation of protein C [18, 19]. At saturating concentrations (0.5 mM) of phospholipids (Table 1, Figure 2) the value of k_{cat}/K_m for protein C activation increases nearly 50-fold (Figure 3) while no effect is observed for cleavage of fibrinogen or PAR1. Phospholipids select the substrate preference of Mz by favoring activation of protein C, but have no significant effect on the activity of thrombin [18, 19] that lacks the Gla domain.

Unlike thrombin, Mz shows an intrinsic propensity to cleave protein C at rates comparable to those of fibrinogen and PAR1 (Table 1, Figure 2) and are further enhanced by the presence of saturating concentrations of phospholipids (Figure 3). This prompted construction of the double mutant W547A/E549A in the Mz_{4R} background. The equivalent double substitution in thrombin is W215A/E217A (WE), which drastically compromises fibrinogen and PAR1 cleavage with minimal effects on the rate of protein C activation in the presence of thrombomodulin [34]. The WE mutant has been studied extensively [28, 35,

Table1: Specificity constants for the hydrolysis of natural substrates under physiological conditions.

Enzyme	Fibrinogen k_{cat}/K_m ($mM^{-1}s^{-1}$)	PAR1 k_{cat}/K_m ($mM^{-1}s^{-1}$)	Protein C[1] k_{cat}/K_m ($mM^{-1}s^{-1}$)
Mz_{4R}	540 ± 48	5000 ± 210	65 ± 0.3
Mz_{4R} (+PL)[2]	400 ± 28	3700 ± 150	2400 ± 51
$Mz_{4R/WE}$	0.23 ± 0.01	7 ± 0.3	0.45 ± 0.002
$Mz_{4R/WE}$ (+PL)[2]	0.44 ± 0.04	11 ± 0.3	72 ± 1
Thrombin[3]	17000 ± 1000	32000 ± 2000	220 ± 10
WE Thrombin[3]	0.25 ± 0.02	10 ± 1	33 ± 2

[1] In the presence of 200 nM rabbit thrombomodulin
[2] 0.5 mM phospholipids
[3] Values from Ref. [45]

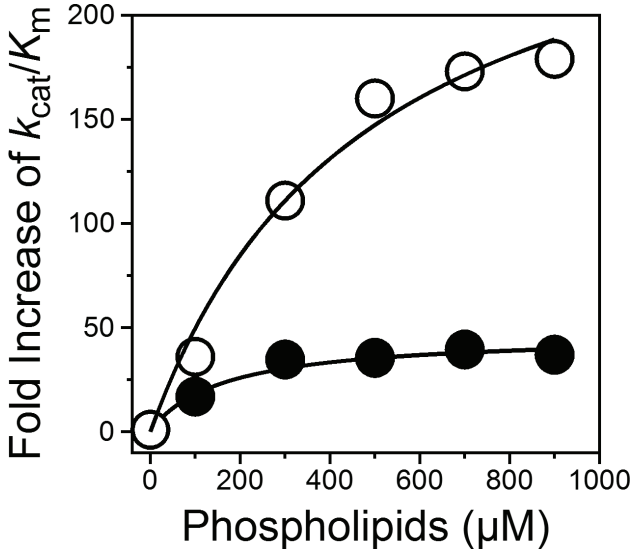

Figure 3. Effect of phospholipids on the rates of protein C activation. The fold increase of the k_{cat}/K_m value for activation of protein C by Mz_{4R} (closed circles) or $Mz_{4R/WE}$ (open circles) relative to the absence of phospholipids is plotted as a function of phospholipid concentrations. The fold increase at saturating concentrations of phospholipids is 47±4 for Mz_{4R} and 290±60 for $Mz_{4R/WE}$, with apparent K_d values of 0.16±0.05 mM and 0.5±0.2 mM, respectively. Experimental conditions are: 145 mM NaCl, 5 mM $CaCl_2$, 0.1% PEG8000, 20 mM Tris, pH 7.5 at 37 °C.

36], features effective anticoagulant and antithrombotic activities *in vivo* [37-39] and is currently in Phase I for the treatment of thrombotic complications and stroke. There is interest to further improve on the properties of WE under conditions that are clinically relevant, and recent studies in murine models supports Mz as a potential scaffold [20, 21]. As expected, the W547A/E549A substitution in Mz_{4R} ($Mz_{4R/WE}$) demonstrates a drastic loss of specificity toward fibrinogen and PAR1. The mutant also presents a significant (140-fold) loss of activity toward protein C that is, however, corrected almost entirely in the presence of saturating concentrations of phospholipids (Table 1, Figures 2 and 3). Under these conditions, $Mz_{4R/WE}$ has highest specificity toward protein C with a value of k_{cat}/K_m that exceeds those of fibrinogen and PAR1 by 160-fold and nearly 10-fold, respectively. This is a notable difference over the WE mutant of thrombin that is borne out by the specific effect of phospholipids on the Gla domain of Mz. Forthcoming studies of $Mz_{4R/WE}$ in non-human primates will reveal how effective this construct may be as an anticoagulant and antithrombotic agent *in vivo*.

Materials And Methods

PCR mutagenesis and Protein Overexpression and Purification

All mutations reported in this study were introduced into the human prothrombin gene sub-cloned in a pDEST40 vector using the Quick-Change Lightning site-directed mutagenesis kit (Agilent Technologies). Plasmids carrying the desired prothrombin mutations were transfected into baby hamster kidney (BHK) cells using Lipofectamine 3000 (Invitrogen) according to a standard protocol supplied by the manufacturer. Stably expressing clones were selected by applying selection pressure with 1.5 mg/mL geneticin, and once the expression was verified through Western blotting, the cells were transferred into large cell factories. Prothrombin was then purified using immuno- and ion-exchanged chromatography as previously described [40]. The selective conversion of prothrombin to Mz was accomplished by overnight incubation of the zymogen at room temperature in the presence of 2 units Ecarin (Sigma-Aldrich) per mg of protein, under these experimental

conditions: 80 mM NaCl, 5 mM $CaCl_2$, 20 mM benzamidine, 20 mM Tris, pH 7.5. Formation of Mz was verified by SDS-PAGE analysis, loaded on a Q-sepharose (GE Healthcare) column equilibrated with 80 mM NaCl, 5 mM $CaCl_2$, 20 mM Tris, pH 7.5 and eluted with a 0-1 M NaCl gradient. This step was followed by size-exclusion chromatography on a Superdex 200 column (GE Healthcare).

Preparation of Phospholipid Vesicles

Phospholipid vesicles composed of phosphatidylcholine and phosphatidylserine (Avanti) at 70:30 molar ratio were prepared using the extrusion method as previously described [41]. Phospholipids were suspended in a solution of 145 mM NaCl and 20 mM Tris, pH 7.5 to generate large multilamellar vesicles. After three freeze-thaw cycles, the vesicles were repeatedly extruded on a mini-extruder through a polycarbonate filter composed of 100 nm pores to create uniformly sized unilamellar vesicles.

Kinetic Assays

Formation of activated protein C was monitored by a continuous assay using the chromogenic substrate H-D-Asp-Arg-Arg-*p*-nitroanilide, as previously described [28]. The concentration of human protein C (HaemTech) was maintained at 50 nM, well below the K_m value, to ensure accurate measurement of the k_{cat}/K_m ratio from progress curves analysis. The concentration of rabbit thrombomodulin (HaemTech) was 200 nM. Values of k_{cat}/K_m for the release of fibrinopeptide A from fibrinogen and PAR1 activation were determined as previously reported [28]. Depending on the concentration of phospholipids and enzymatic activity, the final concentration of enzyme ranged from 0.1 to 3 nM for Mz_{4R} and from 10 to 250 nM for $Mz_{4R/WE}$. All kinetic measurements were carried out under these experimental conditions: 145 mM NaCl, 5 mM $CaCl_2$, 0.1% PEG 8000, 20 mM Tris, pH 7.4 at 37 °C.

smFRET Measurements

A proteolytically stable form of Mz carrying the S525A substitution was labeled at the engineered Cys residues in kringle-1 (S120C) and protease domain (S478C) with Alexa Flour 555-C2-maleamide as a donor and Alexa Flour 647-C2 (Invitrogen) as an acceptor, according to an established protocol [12]. Labeling at these positions has no effect on the structural integrity of the protein [12]. The successful incorporation of the probes at the correct positions was validated through proteolytic digestion with coagulation factor Xa, which cleaves at Arg271 and separates kringle-1 from the protease domain leading to loss of FRET signal. FRET measurements of freely diffusing single Mz molecules were carried out on a confocal microscope MicroTime200 using pulsed interleaved excitation (PIE). All measurements were performed at 18 °C for a time period of 40 min, using a protein concentration of 150 pM under these experimental conditions: 145 mM NaCl, 5 mM $CaCl_2$, 0.02% Tween 20, 20 mM Tris, pH 7.5. Titrations with increasing concentrations of substrates were carried out in 8 well chambered coverglasses with borosilicate glass. Raw data were initially processed with the PIE analysis with MATLAB (PAM) software [42]. Bursts with more than 35 photons were integrated into 0.5 ms time bins and histograms were constructed from molecules with labeling stoichiometry (S) in the 0.3-0.7 range. Consequently, donor-only and acceptor-only labeled species, which are respectively characterized with S values of 1 and approximately 0 to 0.25, were excluded from the final analyses. After applying the correct γ-factor and the appropriate correction factors for donor leakage and direct acceptor excitation, the data were exported and fitted to a double Gaussian function using the peak analyzer function in OriginPro 8.1. The fraction of molecules populating either the low or the intermediate FRET conformations at a specific substrate concentration was calculated by dividing the peak area of each FRET population derived from the double Gaussian fit over the sum of the total area of both peaks. The peak area fraction values were then plotted as a function of substrate concentration and fitted to a single site binding model using OriginPro 8.1.

SAXS Measurements

SAXS data were collected at the beamline 12-ID-B of the Advanced Photon Source at the Argonne National Laboratory (Argonne, IL, USA) on prothrombin and Mz. Both proteins carried the S525A substitution to prevent autoproteolytic digestion. Scattered X-rays at 14 keV radiation energy were measured using a Pilatus 2M detector with a sample-to-detector distance of 2 m. A flow cell was used to reduce radiation damage. Thirty images were collected for each sample and buffer blank. The scattering vector $q=4\pi\sin(\theta/2)/\lambda$ is the momentum transfer defined by the scattering angle θ and X-ray wavelength λ. The isotropic 2D images were converted to 1D SAXS profiles, i.e., intensity vs q, followed by

averaging and background subtraction using software packages at the beamline. The radius of gyration, R_g, was determined using the Guinier approximation in the low q region ($qR_g<1.3$) and its linearity served as an initial assessment of data and sample quality. Maximum particle dimension, D_{max}, and distance distribution function, P(r), were calculated using GNOM [43]. The low resolution envelopes were produced using both GASBOR [43] (q up to 0.8 $Å^{-1}$) and DAMMIN [44] (q up to 0.3 $Å^{-1}$) by directly fitting the reciprocal space scattering profile. Twenty models were generated for every calculation and then aligned and averaged using DAMAVER [44]. The results of GASBOR and DAMMIN were very similar but only GASBOR results are reported here. The NSD (normalized spatial discrepancy) value of calculations for prothrombin is approximately 1.5, indicating good convergence for each twenty models. Convergence for Mz calculations had an NSD value of 2.0.

Acknowledgments: This research used resources of the Advanced Photon Source, a U.S. Department of Energy (DOE) Office of Science User Facility operated for the DOE Office of Science by Argonne National Laboratory under Contract No. DE-AC02-06CH11357. This work was supported in part by a Grant from the American Heart Association 15SDG25550094 (NP), and the National Institutes of Health Research Grants HL049413 and HL139554 (EDC).

References

1. Krishnaswamy S: The transition of prothrombin to thrombin. J Thromb Haemost. 2013;11 Suppl 1:265-276.
2. Mann KG, Jenny RJ, Krishnaswamy S: Cofactor proteins in the assembly and expression of blood clotting enzyme complexes. Annu Rev Biochem. 1988;57:915-956.
3. Doyle MF, Mann KG: Multiple active forms of thrombin. IV. Relative activities of meizothrombins. J Biol Chem. 1990;265:10693-10701.
4. Rosing J, Tans G: Meizothrombin, a major product of factor Xa-catalyzed prothrombin activation. Thromb Haemost. 1988;60:355-360.
5. Rosing J, Zwaal RF, Tans G: Formation of meizothrombin as intermediate in factor Xa-catalyzed prothrombin activation. J Biol Chem. 1986;261:4224-4228.
6. Tans G, Janssen-Claessen T, Hemker HC, Zwaal RF, Rosing J: Meizothrombin formation during factor Xa-catalyzed prothrombin activation. Formation in a purified system and in plasma. J Biol Chem. 1991;266:21864-21873.
7. Krishnaswamy S, Mann KG, Nesheim ME: The prothrombinase-catalyzed activation of prothrombin proceeds through the intermediate meizothrombin in an ordered, sequential reaction. J Biol Chem. 1986;261:8977-8984.
8. Brufatto N, Nesheim ME: Analysis of the kinetics of prothrombin activation and evidence that two equilibrating forms of prothrombinase are involved in the process. J Biol Chem. 2003;278:6755-6764.
9. Orcutt SJ, Krishnaswamy S: Binding of substrate in two conformations to human prothrombinase drives consecutive cleavage at two sites in prothrombin. J Biol Chem. 2004;279:54927-54936.
10. Papaconstantinou ME, Gandhi PS, Chen Z, Bah A, Di Cera E: Na+ binding to meizothrombin desF1. Cell Mol Life Sci. 2008;65:3688-3697.
11. Martin PD, Malkowski MG, Box J, Esmon CT, Edwards BF: New insights into the regulation of the blood clotting cascade derived from the X-ray crystal structure of bovine meizothrombin des F1 in complex with PPACK. Structure. 1997;5:1681-1693.
12. Pozzi N, Bystranowska D, Zuo X, Di Cera E: Structural Architecture of Prothrombin in Solution Revealed by Single Molecule Spectroscopy. J Biol Chem. 2016;291:18107-18116.
13. Pozzi N, Chen Z, Di Cera E: How the Linker Connecting the Two Kringles Influences Activation and Conformational Plasticity of Prothrombin. J Biol Chem. 2016;291:6071-6082.
14. Pozzi N, Chen Z, Gohara DW, Niu W, Heyduk T, Di Cera E: Crystal structure of prothrombin reveals conformational flexibility and mechanism of activation. J Biol Chem. 2013;288:22734-22744.
15. Pozzi N, Chen Z, Pelc LA, Shropshire DB, Di Cera E: The linker connecting the two kringles plays a key role in prothrombin activation. Proc Natl Acad Sci U S A. 2014;111:7630-7635.
16. Chinnaraj M, Chen Z, Pelc LA, Grese Z, Bystranowska D, Di Cera E *et al*: Structure of prothrombin in the closed form reveals new details on the mechanism of activation. Sci Rep. 2018;8:2945.
17. Cote HC, Stevens WK, Bajzar L, Banfield DK, Nesheim ME, MacGillivray RT: Characterization of a stable form of human meizothrombin derived from recombinant prothrombin (R155A, R271A, and R284A). J Biol Chem. 1994;269:11374-11380.
18. Cote HC, Bajzar L, Stevens WK, Samis JA, Morser J, MacGillivray RT *et al*: Functional characterization of recombinant human meizothrombin and Meizothrombin(desF1). Thrombomodulin-dependent activation of protein C and thrombin-activatable fibrinolysis inhibitor (TAFI), platelet aggregation, antithrombin-III inhibition. J Biol Chem. 1997;272:6194-6200.
19. Koike H, Okuda D, Morita T: Mutations in autolytic loop-2 and at Asp554 of human prothrombin that enhance protein C activation by meizothrombin. J Biol Chem. 2003;278:15015-15022.
20. Shim K, Zhu H, Westfield LA, Sadler JE: A recombinant murine meizothrombin precursor, prothrombin R157A/R268A, inhibits thrombosis in a model of acute carotid artery injury. Blood. 2004;104:415-419.
21. Shaw MA, Kombrinck KW, McElhinney KE, Sweet DR, Flick MJ, Palumbo JS *et al*: Limiting prothrombin activation to meizothrombin is compatible with survival but significantly alters hemostasis in mice. Blood. 2016;128:721-731.
22. Hackeng TM, Tans G, Koppelman SJ, de Groot PG, Rosing J, Bouma BN: Protein C activation on endothelial cells by prothrombin activation products generated in situ: meizothrombin is a better protein C activator than alpha-thrombin. Biochem J. 1996;319 (Pt 2):399-405.
23. Tans G, Nicolaes GA, Thomassen MC, Hemker HC, van Zonneveld AJ, Pannekoek H *et al*: Activation of human factor V by meizothrombin. J Biol Chem. 1994;269:15969-15972.

24. von dem Borne PA, Mosnier LO, Tans G, Meijers JC, Bouma BN: Factor XI activation by meizothrombin: stimulation by phospholipid vesicles containing both phosphatidylserine and phosphatidylethanolamine. Thromb Haemost. 1997;78:834-839.
25. Petrovan RJ, Govers-Riemslag JW, Nowak G, Hemker HC, Tans G, Rosing J: Autocatalytic peptide bond cleavages in prothrombin and meizothrombin. Biochemistry. 1998;37:1185-1191.
26. Cantwell AM, Di Cera E: Rational design of a potent anticoagulant thrombin. J Biol Chem. 2000;275:39827-39830.
27. Gruber A, Cantwell AM, Di Cera E, Hanson SR: The thrombin mutant W215A/E217A shows safe and potent anticoagulant and antithrombotic effects in vivo. J Biol Chem. 2002;277:27581-27584.
28. Marino F, Pelc LA, Vogt A, Gandhi PS, Di Cera E: Engineering thrombin for selective specificity toward protein C and PAR1. J Biol Chem. 2010;285:19145-19152.
29. Chakraborty P, Acquasaliente L, Pelc LA, Di Cera E: Interplay between conformational selection and zymogen activation. Sci Rep. 2018;8:4080.
30. Huber R, Bode W: Structural basis of the activation and action of trypsin. Acc Chem Res. 1978;11:114-122.
31. Vogt AD, Chakraborty P, Di Cera E: Kinetic Dissection of the Pre-existing Conformational Equilibrium in the Trypsin Fold. J Biol Chem. 2015;290:22435-22445.
32. Stevens WK, Cote HF, MacGillivray RT, Nesheim ME: Calcium ion modulation of meizothrombin autolysis at Arg55-Asp56 and catalytic activity. J Biol Chem. 1996;271:8062-8067.
33. Sadler JE: Thrombomodulin structure and function. Thromb Haemost. 1997;78:392-395.
34. Cantwell AM, Di Cera E: Rational design of a potent anticoagulant thrombin. J Biol Chem. 2000;275:39827-39830.
35. Gandhi PS, Page MJ, Chen Z, Bush-Pelc LA, Di Cera E: Mechanism of the anticoagulant activity of the thrombin mutant W215A/E217A. J Biol Chem. 2009;284:24098-24105.
36. Pineda AO, Chen ZW, Caccia S, Cantwell AM, Savvides SN, Waksman G *et al*: The anticoagulant thrombin mutant W215A/E217A has a collapsed primary specificity pocket. J Biol Chem. 2004;279:39824-39828.
37. Berny MA, White TC, Tucker EI, Bush-Pelc LA, Di Cera E, Gruber A *et al*: Thrombin mutant W215A/E217A acts as a platelet GpIb antagonist. Arterioscler Thromb Vasc Biol. 2008;18:329-334.
38. Gruber A, Cantwell AM, Di Cera E, Hanson SR: The thrombin mutant W215A/E217A shows safe and potent anticoagulant and antithrombotic effects in vivo. J Biol Chem. 2002;277:27581-27584.
39. Gruber A, Marzec UM, Bush L, Di Cera E, Fernandez JA, Berny MA *et al*: Relative antithrombotic and antihemostatic effects of protein C activator versus low molecular weight heparin in primates. Blood. 2007;109:3733-3740.
40. Guinto ER, Vindigni A, Ayala YM, Dang QD, Di Cera E: Identification of residues linked to the slow-->fast transition of thrombin. Proc Natl Acad Sci U S A. 1995;92:11185-11189.
41. Mui B, Chow L, Hope MJ: Extrusion technique to generate liposomes of defined size. Methods Enzymol. 2003;367:3-14.
42. Schrimpf W, Barth A, Hendrix J, Lamb DC: PAM: A Framework for Integrated Analysis of Imaging, Single-Molecule, and Ensemble Fluorescence Data. Biophys J. 2018;114:1518-1528.
43. Svergun DI, Petoukhov MV, Koch MH: Determination of domain structure of proteins from X-ray solution scattering. Biophys J. 2001;80:2946-2953.
44. Svergun DI: Restoring low resolution structure of biological macromolecules from solution scattering using simulated annealing. Biophys J. 1999;76:2879-2886.
45. Wood DC, Pelc LA, Pozzi N, Wallisch M, Verbout NG, Tucker EI *et al*: WEDGE: an anticoagulant thrombin mutant produced by autoactivation. J Thromb Haemost. 2015;13:111-114.